

NUMERICAL SIMULATION OF EXPERIMENTS ON MASONRY ARCH BRIDGES

C. Molins¹, P. Roca², O. Arnau³, R. Farina⁴

¹ Associate Professor. Department of Civil & Environmental Engineering, Universitat Politècnica de Catalunya, SPAIN.

² Professor. Department of Civil & Environmental Engineering, Universitat Politècnica de Catalunya (UPC), SPAIN.

³ Ph.D. Structural Engineer, SPAIN.

⁴ M.Sc. Structural Engineer, SPAIN.

e-mails: climent.molins@upc.edu, pere.roca.fabregat@upc.edu, oriol@oriolarnau.com, rafael.farina@usp.br

SUMMARY

The paper describes the numerical simulation of the loading tests up to failure carried out on a short-span, true-scale brick masonry arch bridge. The research was aimed at assessing the capability of different approaches on reproducing the real structural response presented along – the whole loading process. The arch was tested at the Universitat Politècnica de Catalunya (UPC), collecting all the necessary data related to the materials properties and the test procedures, and registering the obtained experimental results. In this paper, the bi-dimensional finite elements simulations with appropriate constitutive equations for the materials are presented, covering: the brick masonry, the sand infill and the interfaces between infill and masonry.

Keywords: *Numerical simulation, masonry arch bridge, structural capacity.*

1. INTRODUCTION

Masonry arch bridges represent an integrant part of the European roadway and railway networks. Therefore, it is necessary to accurately assess their response and strength against new demands of loads, traffic and standards.

Based on an experimental research of a real-scale segmental arch bridge performed at the Laboratory of Structural Technology at the Department Civil and Environmental Engineering of UPC – Barcelona Tech, the present work aims to evaluate the quality of the assessment provided by the use of the Finite Element Method using macro models with discontinuities, particularly in terms of collapse mechanism and ultimate capacity.

Finite element method is a powerful tool when applied to masonry arch bridges, providing a general understanding of the governing collapse mechanisms. However obtaining accurate results of ultimate capacity and detailed collapse mechanism in regard to experimental evidence demands a deep knowledge of the materials behaviour and the constitutive models to be used.

For this work mostly plane stress models with nonlinear homogenous materials and discontinuities modelled with interface elements were analysed. In addition, a sensitivity

analysis of the models to the variation of particular parameters not experimentally determined is performed. Finally, a discussion about the modelling assumptions is presented.

2. DESCRIPTION OF THE EXPERIMENTAL ARCHES

The experimental model, depicted in Fig. 1, is a segmental arch masonry bridge built over reinforced concrete footings simply supported on the ground. Main geometrical properties of the tested bridge are summarized in Tab. 1.

Steel plates stiffened with steel profiles were installed at the back sides of the abutments to retain the infill (Fig. 2), and a set of ties, consisting of steel bars with a diameter of 25 mm, were anchored to the horizontal profiles stiffening the plates. The vertical position of the pair of ties in relation to the ground is approximately 0.05m, 0.35m and 0.55m and 0.85m respectively. The total weight of the bridge was approximately 70 kN.

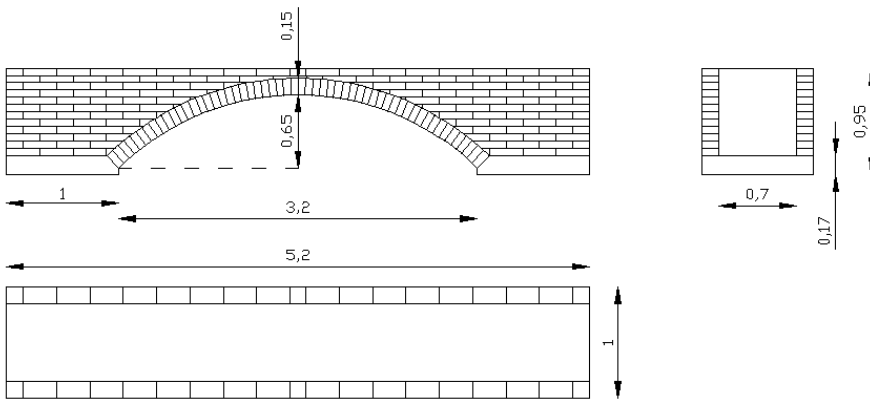


Fig. 1. Front, section and plan view of the bridge [1].

Table 1. Main geometrical parameters of the bridge.

| Geometrical parameter | |
|---|-----------------------|
| type | segmental |
| free span (m) | 3.20 m |
| rise (m) | 0.65 m |
| total length (with abutments) (m) | 5.20 m |
| total height (m) | 0.95 m |
| width (m) | 1.00 m |
| ring depth (m) | 0.15 m |
| depth of infill on crown (m) | 0.10 m |
| maximum depth of un-cohesive infill (m) | 0.78 m |
| thickness of spandrel walls (m) | 0.15 m |
| thickness of concrete footing | 0.20 m |
| number of steel ties ($\phi=25$ mm) | 8 |
| loaded point | $\frac{1}{4}$ of span |



Fig. 2. Steel plates confining the infill and the ties balancing the plates.

The brick masonry was built with units measuring 13.5×28.5×4.5 cm and bed joints 1-1.5 cm thick. The same type of M8 Portland cement mortar was used for the ring of the arch, the walls of spandrels and buttresses. The infill consisted of compacted sand with 6% moisture contents and specific weight of 18 kN/m³ (dry specific weight of 15.55 kN/m³).

Tab. 2 shows the experimental material properties of elementary mortar, brick and of masonry prism specimens. In particular, the properties of the mortar-unit interface were determined by testing couplets with a biaxial testing equipment.

Detailed explanation of the tests results and a preliminary assessing using limit analysis of the results were already presented in [1].

Table 2. Experimental material properties of masonry components and composite.

| Component | Property | Average (N/mm ²) | Type of specimen |
|--------------------|-------------------------|------------------------------|-----------------------------|
| Brick (lengthwise) | Compression strength | 56.8 | 40x40x120 mm prisms |
| | Young modulus | 12,750 | |
| Brick (flatwise) | Compression strength | 51.0 | 3 stacked 40 mm cubes |
| | Young modulus | 10,450 | |
| Mortar | Compression strength | 8.34 | Prismatic 40×40×80 mm |
| | Flexural strength | 2.68 | Prismatic 40×40×160 mm |
| | Young modulus | 810 | |
| Joint interface | Cohesion | 0.33 | couplet (biaxial equipment) |
| | Initial friction angle | 45° | “ |
| | Residual friction angle | 37.2° | “ |
| Masonry | Compression strength | 21.0 | 4 flat brick prism |
| Infill (sand) | Specific weight | 18 kN/m ³ | |

3. MODELIZATION

Macro-models encounter a significant limitation in their inability to simulate strong discontinuities between different blocks or parts of the masonry construction. Such discontinuities, corresponding either to physical joints or individual cracks formed later in the structure, may experience phenomena such as block separation, rotation or frictional sliding, which are not easily describable by means of a FEM approach strictly based on continuum mechanics. A possible way of overcoming these limitations consists of the inclusion within the FEM mesh of joint interface elements to model the response of discontinuities. All the numerical results presented in this paper were obtained using Diana (version 9.6) software [2].

Therefore, the macro-modelling material technique with model discontinuities [3] is used in order to simulate the experiments. Interface elements are placed between the infill and the other elements, namely confinement steel plates, concrete slabs and arch ring.

Steel of the ties and concrete of the footings were modelled as linear elastic materials because their stress state was far from yielding. Non-linear springs (zero tension) were considered in the footing supports in order to allow the local lifting.

3.1. Masonry model

The material model used to describe the non-linear behaviour of the masonry is a smeared cracking model based on total strain, also called the 'Total Strain rotating crack model', which describe the tensile and compressive behaviour of a material with one stress-strain relationship. This type of models is very well suited for Serviceability Limit State (SLS) and Ultimate Limit State (ULS) analyses which are predominantly governed by cracking or crushing of the material which is the case of masonry.

The tensile behaviour is described by an exponential tension softening function, based on the tensile strength fracture energy and crack bandwidth. The Compression (crush) behaviour is defined by a parabolic function set up with compression strength, compressive fracture energy and crack bandwidth. For all models the compressive strength of the masonry was set as $f_c = 21 \text{ N/mm}^2$, according to the experiments and the compressive fracture energy (G_c) to 5 N/mm .

3.2. Soil model

The Mohr-Coulomb yield condition is the constitutive model assigned to the infill in all models, set up with cohesion c , friction angle Φ , and dilatancy angle ψ parameters, the last adopted equal to the friction angle assuming associated plasticity. Although hardening and tension cut-off are available in this model, they were not applied.

3.3. Interface model

The interface behaviour was modelled according to the coulomb friction criterion (Fig. 3). The non-linear parameter set up for the interface were cohesion c , friction angle Φ , and dilatancy angle ψ .

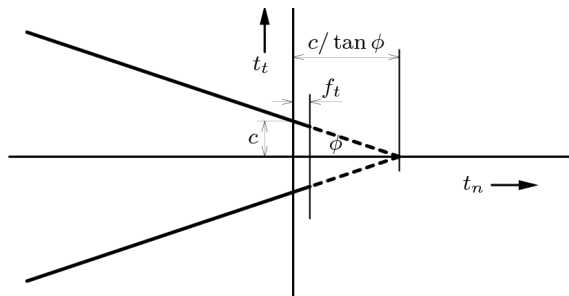


Fig. 3. Coulomb friction criterion.

3.4. Loading process

In the experiment, the live load was applied by a vertical actuator on a concrete block of 20x20cm section lying on the infill at $\frac{1}{4}$ of the span. Consistently, in the simulations dead load was applied in a first stage and, then, the live load was applied using displacement control on the concrete block.

4. RESULTS

2D models can provide a good approach to the real behaviour and capacity of real arches. However, in this particular tested bridge, where the spandrel walls account for almost 30% of the overall width, both the infill and the spandrel walls are very important in the structural response.

Realizing that 2D models are easier to prepare, faster to analyse, and helpful to better understand the interaction between the infill and the arch vault, most of the analyses were developed using 2D models. Several sensitivity analyses were performed in order to find appropriate parameters for some of the variables without experimental determination such as; soil cohesion –which had to be very limited in a sand soil-, fracture energy and tensile strength of masonry, and interface properties between the soil and the arch ring.

4.1. Sensitivity analysis

4.1.1. Infill cohesion

One of the main difficulties to simulate the infill in a masonry arch bridge is that normally it is very difficult to have the properties of that infill. In safety checks this can be solved with safe assumptions, i.e. in a segmental arch taking into account only the weight of the infill. However, in semi-circular arches the confinement effect of infill cannot be neglected, especially when the aim is the realistic simulation of experiments. Fig. 4 shows the dramatic effect of the cohesion in the capacity of the arch. The minimum value displayed in Fig. 4 is the minimum value that produced converged results in the analyses.

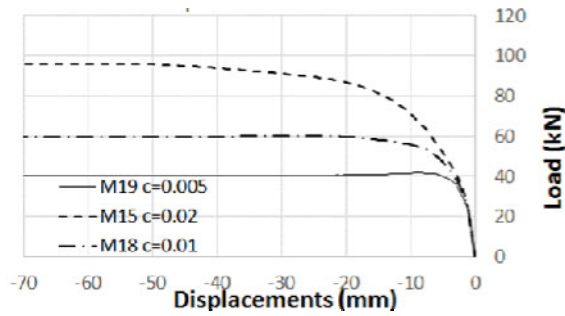


Fig. 4. Load vs vertical displacement at $L/4$ for different soil cohesion values in N/mm^2 .

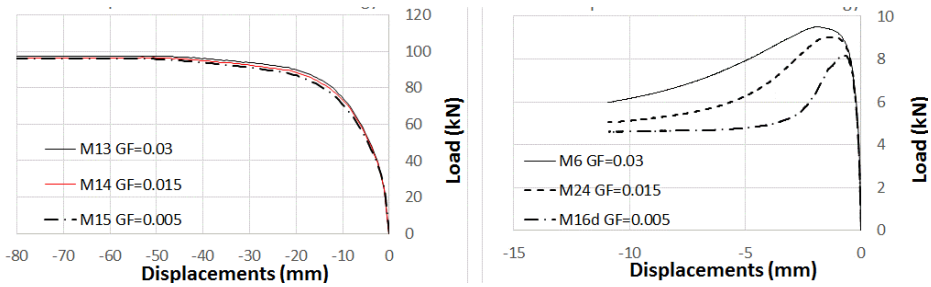


Fig. 5. Load vs vertical displacement at $L/4$ for different fracture energy values for a 2D model with (left) or without infill (right).

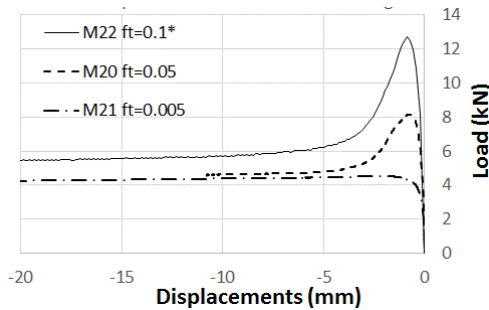


Fig. 6. Load vs vertical displacement at $L/4$ for different tensile strength values for a 2D model without infill.

4.1.2. Fracture energy and tensile strength of masonry of the arch

Different values of the fracture energy and tensile strength of the masonry were tested for models with and without soil (and interface elements between the ring and the infill). It can be appreciated in Fig. 5 that the effect of fracture energy on the ultimate capacity

is very limited in both cases. However it affects the post-peak behavior of the cracks in the masonry, what can be particularly assessed when observing the softening branches after the peak load in the model without soil. The plateau in the complete model is a consequence of soil yielding in the longitudinal direction of the bridge.

The ultimate capacity is sensitive to the tensile strength of masonry of the ring, particularly in the case of the arch without infill as it is shown in Fig. 6.

4.1.3. Interface cohesion and stiffness

The properties of the interface were obtained according to the recommendations of CUR report [4] for joints in masonry, assuming the particular properties of brick and mortar presented in Tab. 1. The influence of the interfaces cohesion and stiffness is presented in Fig. 7. As it can be appreciated, both parameters affect less than 10% the ultimate load of the structure. During the experiment, separation of the arch ring and the spandrel walls was observed [1]. However, the plane stress model with the infill cannot reproduce such effect because the infill between the loaded block and the arch ring is subjected to compression forces and detachment between them is not possible.

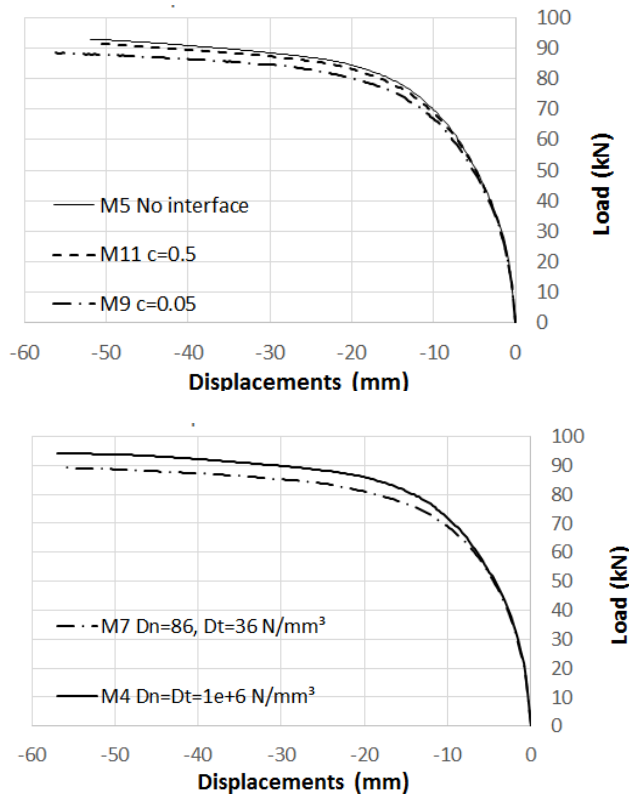


Fig. 7. Load vs vertical displacement at L/4 for different interface cohesion (above) and stiffness (below).

4.2. Comparison with experiment

In this section the best fitting result obtained using the 2D model is presented. Fig. 8 shows both the numerical and the experimental load displacement diagrams presenting a very similar overall behavior. Both diagrams present a change of slope in the beginning of the loading and a second just before the ultimate load, indicating a similar collapse mechanism. Indeed, in Fig. 9 the crack strains on the arch ring prove the formation of four hinges, as in the experiment [1].

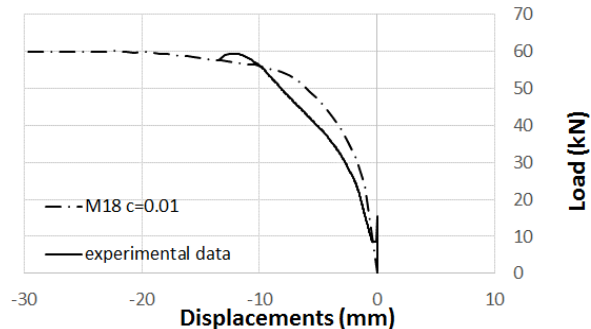


Fig. 8. Numerical and experimental load - vertical displacement diagrams at L/4.

However, the load-displacement diagram of the model, Fig. 8, presents a third change in the slope, just before the plateau, while the experimental curve abruptly starts unloading, denoting the full development of the hinges. This plateau is very likely to be related to the plasticization of the soil (with unrealistic softening). Fig. 10 displays the principal strains of the model corresponding to this last change of slope, at around 20mm of applied displacement.

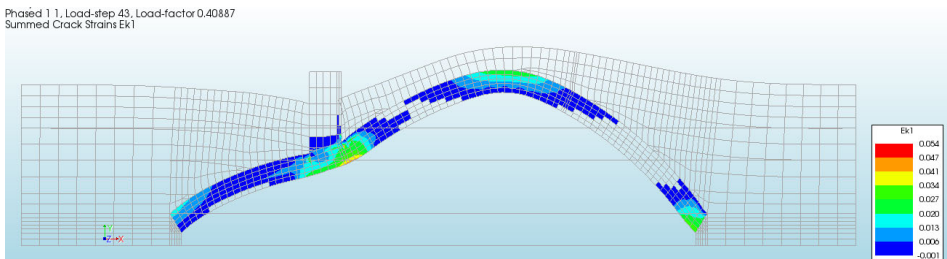


Fig. 9. Crack strains on the arch ring at 20 mm vertical displacement.

The comparison of forces in the ties of the model with the experimental ones is displayed in Fig. 11. Despite the gap between the experimental and numerical results, qualitatively the development of the forces are similar, the upper ties are both less tensioned and are less sensible to the load increment while the lower ties are more tensioned and are more sensitive to the load increment.

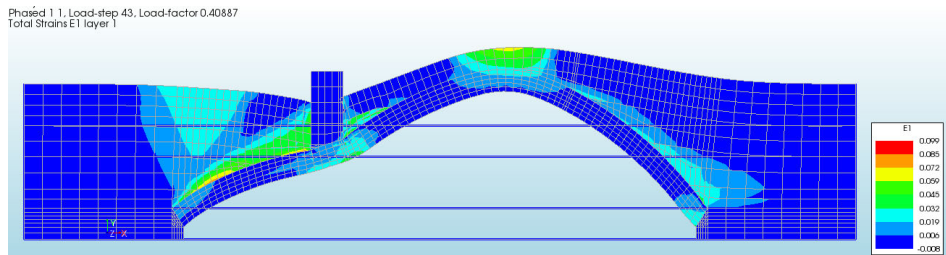


Fig. 10. Total strains on the bridge at 20 mm vertical displacement.

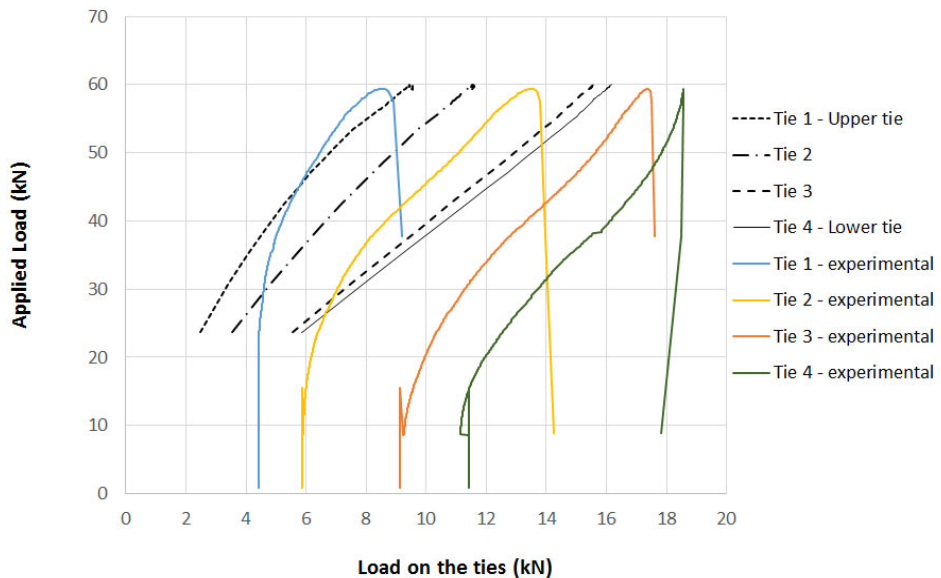


Fig. 11. Numerical and experimental diagrams of load vs force in the ties.

It is worth to note that the use of a soil model without hardening in compression implied to model the area under the load as masonry to allow the continuation of the analysis (Fig. 9 and Fig. 10). Despite this configuration is not the most realistic as it affects the distribution of the load over the extrados of the arch, it provided satisfactory results regarding the deformed shape and ultimate load.

5. CONCLUSIONS

The paper presents 2D FE simulations of an arch bridge that was tested up to failure. The simulation has been based on a total strain model allowing the description of cracking in tensions (by means of an smeared approach) and yielding-crushing in compression. The contact between the infill and the masonry elements has been modelled by means of

interface elements able to describe separation and frictional sliding. The simulation of the response of a masonry arch using this type of sophisticated model requires significant effort to characterize experimentally the mechanical parameters needed as input data.

The analyses performed showed that the properties of the material of the infill influenced the behaviour of the model either in the loading process, the ultimate load and the post-peak behaviour. A simplified soil model, without hardening in compression or tension cut-off, provides inaccurate results.

ACKNOWLEDGMENTS

This research has received the financial support from the *Ministerio de Economía y Competitividad* of the Spanish Government and FEDER EU funds through the research project MULTI-MAS (Multiscale techniques for the experimental and numerical analysis of the reliability of masonry structures, ref num. BIA2015-63882-P).

REFERENCES

- [1] ROCA P. and MOLINS C., Experiments on Arch Bridges, *ARCH'04*, Barcelona, 2004, pp. .
- [2] TNO DIANA BV., *DIANA 9.6 User's Manual*, TNO DIANA BV, Delft, 2014.
- [3] ROCA P., CERVERA, P., GARIUP, G. and PELÀ, L., Structural analysis of masonry historical constructions. Classical and advanced approaches, *Archives of Computational Methods in Engineering*, Vol. 17, 2010, pp. 299-325
- [4] CUR, *Structural Masonry, an Experimental/Numerical Basis for Practical Design Rules*, A.A.Balkema, Rotterdam, 1997.